

## Article

# Experimental Study on the Potential Utilization of Olive Oil Production Wastes and By-Products as Building Materials

Alexandre Jerónimo <sup>1</sup>, Mariana Fernandes <sup>1,2</sup>  and Ana Briga-Sá <sup>1,3,\*</sup> 

<sup>1</sup> CQ-VR-Centre of Chemistry of Vila Real, University of Trás-os-Montes e Alto Douro, 5000-801 Vila Real, Portugal; ajaj@utad.pt (A.J.); mspf@utad.pt (M.F.)

<sup>2</sup> Department of Chemistry, University of Trás-os-Montes e Alto Douro, 5000-801 Vila Real, Portugal

<sup>3</sup> ECT-School of Science and Technology, University of Trás-os-Montes e Alto Douro, 5000-801 Vila Real, Portugal

\* Correspondence: anas@utad.pt

**Abstract:** The construction industry is one of the sectors with the greatest environmental impact resulting from the high consumption of resources and the huge amount of waste generated. In addition, different wastes and by-products originate from various sectors of activity, namely the ones related to the agricultural sector, requiring the urgent actions of recycling and reuse. In this context, this investigation focused on the valorization of wastes and by-products resulting from the olive oil production as building material components. Wet bagasse was added to cementitious mixtures at percentages of 5% and 20% to produce solid blocks. Lime mortars, incorporating 2% and 8% of ash, were developed, and particleboards composed of 83% olive stone were also produced. The results showed that blocks with 5% waste complied with the standard requirements for flexural strength. The incorporation of 2% ash increased the mechanical properties of lime mortars when compared to a reference mortar with no ash. The developed particleboards revealed the possibility for being part of a multilayer solution or as a covering material, presenting a thermal conductivity of 0.08 W/mK. Thus, wastes generated during olive oil production presented potential for valorization as building material components for non-structural purposes.

**Keywords:** building materials; olive oil wastes; wastes valorization; sustainability



**Citation:** Jerónimo, A.; Fernandes, M.; Briga-Sá, A. Experimental Study on the Potential Utilization of Olive Oil Production Wastes and By-Products as Building Materials. *Sustainability* **2024**, *16*, 1355. <https://doi.org/10.3390/su16041355>

Academic Editor: Asterios Bakolas

Received: 10 November 2023

Revised: 23 January 2024

Accepted: 2 February 2024

Published: 6 February 2024



**Copyright:** © 2024 by the authors. Licensee MDPI, Basel, Switzerland. This article is an open access article distributed under the terms and conditions of the Creative Commons Attribution (CC BY) license (<https://creativecommons.org/licenses/by/4.0/>).

## 1. Introduction

According to United Nations (UN) reports, the world population will reach 9.7 billion people by 2050 [1]. This population growth is intrinsically linked to an increase in quality-of-life requirements and rapid urbanization, consequently leading to harmful impacts on the environment, concerning climate change, resource scarcity, and waste generation. Considering this scenario, human well-being, environmental sustainability, and economic growth are fundamental concerns requiring urgent actions and strategies across diverse economic activities. The construction sector plays an important role in this context, contributing significantly to the consumption of energy and raw materials, waste production, and, consequently, CO<sub>2</sub> emissions. At the same time, it can represent a valuable contribution to the valorization of wastes and by-products as innovative building material components, complying with sustainability and circular economy principles and pursuing European targets in this field. This situation has encouraged the scientific community to develop more effective and environmentally friendly solutions, reducing waste or, alternatively, introducing it into the value chain with new uses. In addition to the construction sector, a large amount of wastes and by-products result from agroforestry activities, which are not given new uses and whose final destination is usually landfill or incineration [2]. In this context, several studies have emerged in order to analyze the potential valorization of agro-wastes, whether or not subjected to transformation processes. Materials such as sugarcane bagasse, banana leaves ashes, bamboo leaf, jute fiber, groundnut shell, wooden mill waste, coconut,

rice husk, and cotton stalk, have been studied as components for bricks, particleboards, acoustic, insulation, and reinforcement materials [3–19]. Previous research in this field also shows that the physical, chemical, and mechanical properties of these innovative materials can lead to a wide variation in performance, meaning further studies should be conducted to optimize mixture compositions depending on waste availability and the required application. Thus, the introduction of other types of agroforestry by-products and wastes as building material components, without being subjected to physical–chemical transformation processes such as incineration, should be highlighted. Furthermore, several wastes and by-products are generated at various stages of agro-industrial activities, and their potential for recovery in the construction sector justifies more investigation, as is the case of those resulting from olive oil production.

In Mediterranean countries, economic activities related to olive cultivation and olive oil production play an extremely important role at social and economic levels. Olives and olive oil are the basis of the Mediterranean diet, responsible for the generation of employment and the decrease in rural depopulation [20]. In the last decades, the olive oil market has grown exponentially, increasing from 1.4 million tons in 1990/1991 to 3.2 million tons in 2015/2016, and a decrease in production is not expected, given the nutritional and economic benefits [21]. In Portugal, around 136,000 tons of olives were produced in 2021, of which 110,000 tons were produced only in the Trás-os-Montes and Alto Douro regions [22]. However, the olive oil industry generates huge amounts of highly polluting by-products, namely wastewater and solids [2], whose reintegration in the value-chain should be explored. Olive bagasse is a result of this industry, whose production in Portugal is approximately 370,000 tones/year [23]. From the extraction process of wet bagasse, stones, dry bagasse, fats, and wastewater are obtained. Normally, stones are reintroduced into the production process as biomass, resulting in ash. Dried bagasse is usually used as fertilizer, and wastewater treatment is required [23]. Some recovery alternatives for olive oil bagasse include composting, biological treatments, direct combustion for energy production, or direct land application [24]. Research has also concerned the extraction of bioactive phenolic compounds [25] and its application as a biomaterial for tanning leather [24]. Regarding building applications, different studies have emerged, referring to the incorporation of olive oil residues, giving special attention to the addition of ash to cement and cement-lime mixtures [26–33]. Some studies were also found referring to the production of bricks [34,35]. In a recent review study, Abdeliazim et al. [36] analyzed the utilization of olive-stone biomass ash to obtain green concrete, confirming the huge potential of its use as a replacement for natural fine aggregate or as a binder in concrete mixtures. The effects of its addition on workability, setting times, soundness, compressive and flexural strength, shrinkage, and durability were examined, and a comparison to control cement pastes was performed. Workability significantly decreased with the increase in olive waste ash content, and the initial setting time increased when added to the cement paste. Its incorporation as a partial replacement of sand improved the compressive and flexural strength of mortars, while the opposite was verified with its addition as a partial cement replacement. The study also reported that the expansion and density significantly decreased with an increase in ash content, and a reduction in thermal conductivity was also achieved. However, recommendations for further studies are suggested by the authors for a more detailed analysis of its effect on the properties of concrete and mortar mixtures. In addition to the ongoing investigation regarding the utilization of specific olive waste for producing mortars and concrete, more attention should be given to other possibilities of building applications using various types of wastes resulting from olive oil production, such as olive pomace solid aggregates and olive mill wastewater, whose studies are still limited [36–40]. In this context, this investigation aims to contribute to the knowledge in the field by evaluating the potential utilization of various residues and by-products generated during different stages of olive oil production. Thus, wet bagasse, stone, and ash will be studied as building material components to produce solid blocks, particleboards, and mortars, respectively.

This article is structured as follows: first, the characterization of the different olive oil wastes and by-products under study will be performed. Second, the preparation of the samples and the experimental procedure to determine the properties of the mortars, blocks, and particleboards will be described. Third, the main results will be presented and discussed. Finally, the main conclusions will be drawn, and future perspectives will be identified.

## 2. Materials and Sample Preparation

In this section, the main characteristics of the olive oil production wastes and by-products (OW) under study will be presented, and their incorporation as building material components will be described. The experimental procedure to evaluate the physical and mechanical properties of the innovative building materials will also be described.

### 2.1. Characterization of OW

In this research work, three types of OW ( $OW_B$ ,  $OW_S$ , and  $OW_A$ ) will be analyzed, and their obtention process is schematically described in Figure 1. After the harvesting stage, the first step in olive oil production is cleaning the olives and removing the stems, leaves, twigs, and other debris left with the olives. The second step is milling the olives into a paste to tear the flesh cells and facilitate the oil release. Mixing the paste allows small oil droplets to combine into bigger ones. Subsequently, the olive paste undergoes a centrifugation process, where virgin oil is separated from the wet bagasse, which includes olive stones ( $OW_{BS}$ ). The sub-product obtained during this stage undergoes a new centrifugation process, allowing the separation of the wet bagasse ( $OW_B$ ) from the olive stones ( $OW_S$ ). As mentioned previously, the stones are usually reintroduced into the production process as biomass, resulting in ash ( $OW_A$ ). A preliminary characterization regarding elemental chemical composition, microstructure, density, and granulometry was carried out for the various OWs under study.

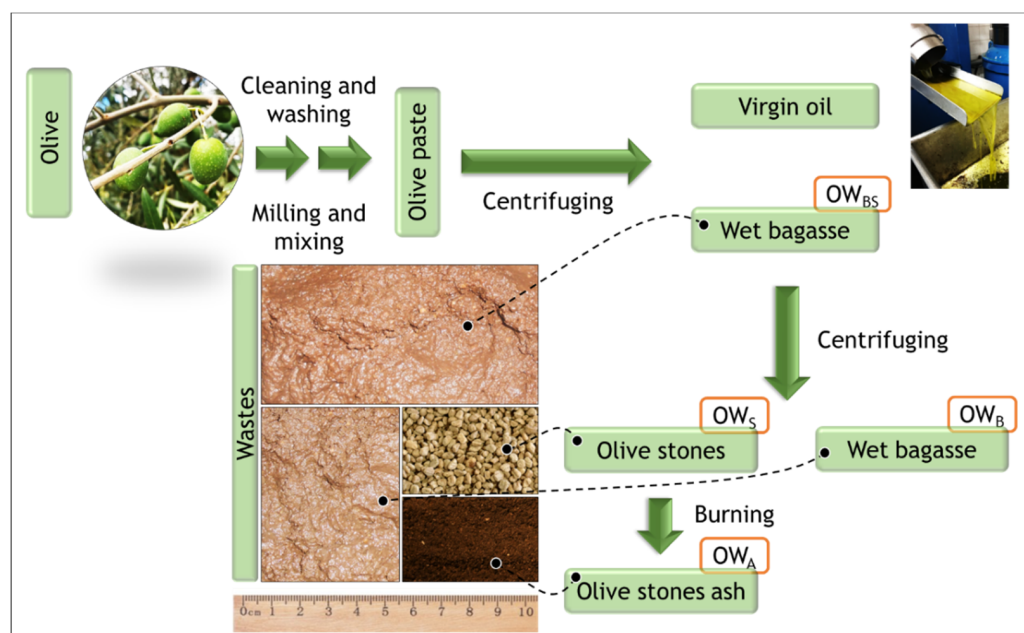


**Figure 1.** Different stages of olive oil production and corresponding OWs under investigation.

$OW_B$  is a brown paste with an intense odor, containing residual quantities of olive stones after the centrifugation process, and presenting a density value around  $1126 \text{ kg/m}^3$ . Its pH value was evaluated using pH strips. Values between 4 and 5 were found, indicating an acidic behavior. This information is especially important when choosing binders that can be employed in mixtures containing these types of residues, suggesting a careful analysis, given that cementitious matrices with acidic waters in the mixture can lead to mechanical

performance decrease [2,41].  $OW_S$  is a homogeneous brown granulated material, with identical aspects to a fine aggregate, whose particle size varies between 1 mm and 4 mm, presenting a density of  $674 \text{ kg/m}^3$ .  $OW_A$  is an ash with a homogeneous and fine grey color, with a particle distribution in a range from 0.063 mm and 2 mm, with a density value of  $311 \text{ kg/m}^3$ .

The chemical characterization allowed us to conclude that all OWs mostly constitute carbon and oxygen.  $OW_A$  is also composed of potassium and calcium in significant amounts, as shown in Table 1. The identification of the elemental chemical composition of these types of agro-wastes is extremely important for further analysis and discussion concerning the chemical reactions that occur when incorporated into mixtures, namely in the presence of common binders such as cement and lime [2]. In Table 1, the elemental chemical composition of each OW is presented.

**Table 1.** Elemental chemical composition of studied OWs.

| OW     | Elemental Chemical Composition [%] |            |
|--------|------------------------------------|------------|
|        | Carbon (C)                         | Oxygen (O) |
| $OW_B$ | 51.4                               | 37.3       |
| $OW_S$ | 52.5                               | 45.2       |
| $OW_A$ | 20.3                               | 27.5       |

The surface morphology of the different OWs was also inspected with a scanning electron microscope (SEM), allowing us to obtain the images shown in Figure 2, revealing a more porous microstructure in the case of the  $OW_A$  sample. This information can be useful for better understanding the physical and mechanical behavior of the developed composite materials.

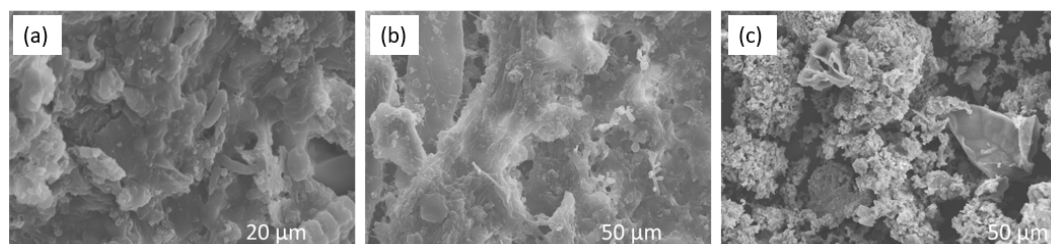


**Figure 2.** SEM images of OWs: (a)  $OW_B$ ; (b)  $OW_S$ ; (c)  $OW_A$ .

## 2.2. Preparation of Samples

In order to analyze the possibility of incorporating these types of wastes into the production of innovative building materials, different mixtures with different percentages of wastes and binders were defined, depending on the materials' purpose, as schematically represented in Figure 3. Taking this into account, preliminary experiments were carried out to evaluate the workability and consistency of the mixtures, depending on the specificities of the studied wastes and the building materials under development. The heterogeneity of wastes led us to consider different contents in the mixtures. In the case of  $OW_B$ , previous experiments showed that higher values of wet bagasse content could be introduced into cement mixtures when compared to the incorporation of  $OW_A$ . Similarly, it was found that introducing larger amounts of ash made workability difficult and affected the samples' integrity [2]. Regarding the use of  $OW_S$ , this by-product was first introduced into a cementitious mixture as a partial replacement of the fine aggregate, revealing, however, a lack of adhesion during the cement hydration process. Thus, an alternative utilization was taken into consideration, using it as a raw material to produce olive stone particleboards. In this case, an attempt was made to maximize the percentage of its content in the mixture for greater valorization of this by-product. The percentage of each OW in the mixtures is presented in Table 2. The formulation of the pastes to produce solid blocks, particleboards,

and mortars is shown in Table 3. A superplasticizer was added to the cementitious and hydraulic-lime pastes to increase workability. The density values of each building material resulting from the incorporation of OW are also included in Table 2. This density refers to the absolute density, which is determined by dividing the mass per unit volume.

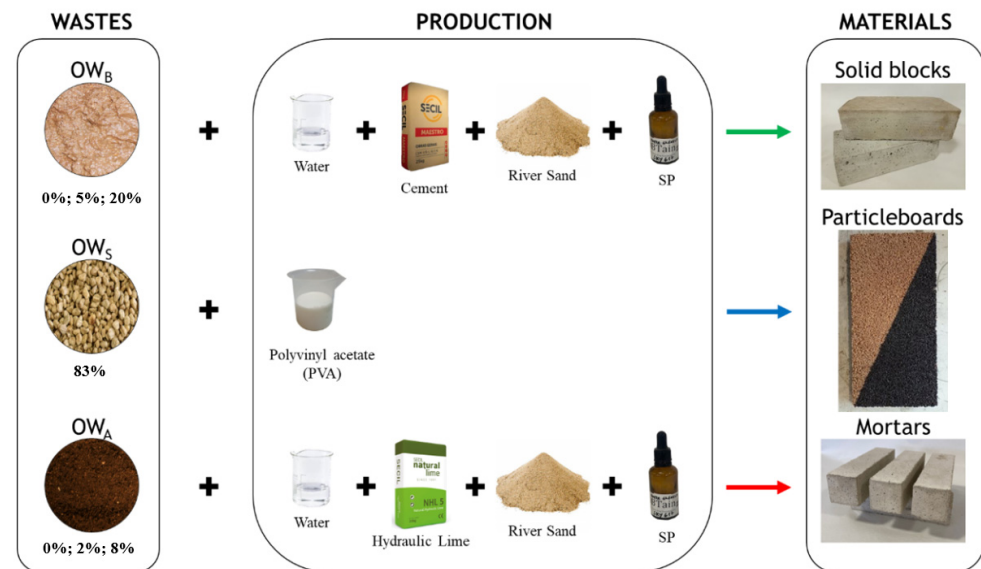


**Figure 3.** Preparation of the mixtures and respective building materials.

**Table 2.** Content of OW in the sample's formulation and respective density.

| OW     | Content [%] | Density [kg/m <sup>3</sup> ] |
|--------|-------------|------------------------------|
| $OW_B$ | 0%          | 2115                         |
|        | 5%          | 2116                         |
|        | 20%         | 1839                         |
| $OW_S$ | 83%         | 755                          |
|        | 0%          | 1813                         |
| $OW_A$ | 2%          | 1753                         |
|        | 8%          | 1673                         |

**Table 3.** Formulation of the mixtures to produce solid blocks, particleboards, and mortars (kg/m<sup>3</sup>).

| Samples    | Binder | Sand    | SP   | OW      | Water  |
|------------|--------|---------|------|---------|--------|
| $OW_B$ 0%  | 500.00 | 1583.16 | 1.00 | 0.00    | 300.00 |
| $OW_B$ 5%  | 500.00 | 1522.64 | 1.00 | 25.00   | 300.00 |
| $OW_B$ 20% | 500.00 | 1341.08 | 1.00 | 100.00  | 300.00 |
| $OW_S$ 83% | 187.00 | -       | -    | 1100.00 | -      |
| $OW_A$ 0%  | 500.00 | 1226.83 | 1.00 | 0.00    | 359.48 |
| $OW_A$ 2%  | 500.00 | 1204.35 | 1.50 | 10.00   | 359.48 |
| $OW_A$ 8%  | 500.00 | 1138.20 | 2.50 | 40.00   | 359.48 |

As mentioned previously, the wet bagasse paste,  $OW_B$ , was introduced into the cementitious mixture as a partial replacement for sand to analyze its suitability in producing solid blocks. For the preparation of the mixture, the following materials were used: Portland cement (2999 kg/m<sup>3</sup>), river natural sand (2322 kg/m<sup>3</sup>), superplasticizer (SP) Master SKY617 (1041 kg/m<sup>3</sup>), and distilled water. Wet bagasse was incorporated into the paste's formulation at percentages of 5% and 20% in relation to the cement content to produce solid blocks with dimensions of 200 mm × 100 mm × 60 mm. A reference sample with no



waste bagasse content was used as a control. The experimental procedure for producing the specimens is shown in Figure 4.

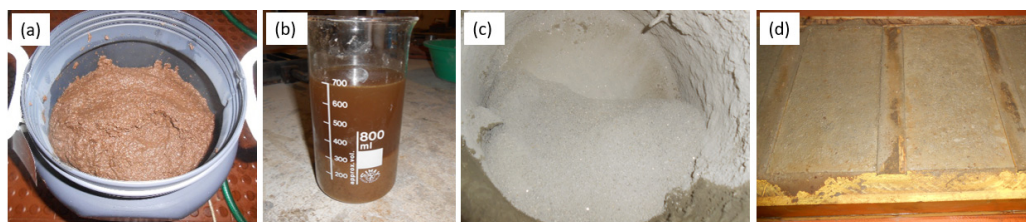


**Figure 4.** Production of  $OW_B$  solid blocks: (a)  $OW_B$ ; (b)  $OW_B$  with distilled water; (c) river sand; (d) molding phase.

As for  $OW_S$ , this waste was reused as a raw material to obtain particleboards with dimensions of 20 mm × 200 mm × 400 mm, using polyvinyl acetate (PVA), an aqueous solvent, as a binder, with a density of 1240.00 Kg/m<sup>3</sup>, water resistance class D2, and pH 6–8. In this case, the particleboards containing 83% of olive stone were subjected to thermal performance evaluation. Figure 5 presents the different stages of the  $OW_S$  particleboards' manufacturing process. The olive stone content was maximized and the binder was minimized, ensuring the workability of the mixture.

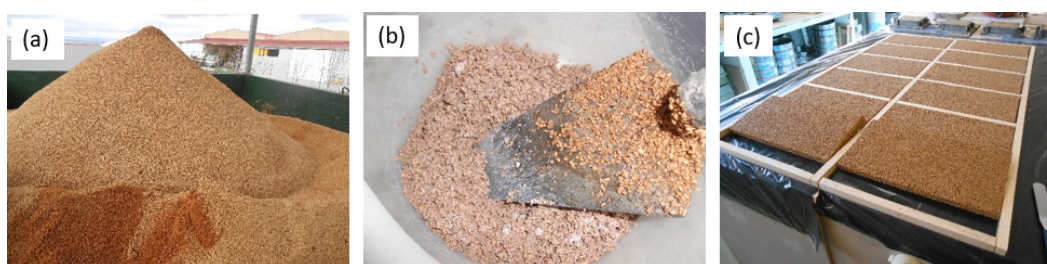


**Figure 5.** Production of  $OW_S$  particleboards: (a)  $OW_S$ ; (b) preparation of the mixture of  $OW_S$  with PVA; (c) molding phase.

Hydraulic-lime mortars were also prepared, considering the addition of  $OW_A$  at percentages of 2% and 8% when compared to the binder percentage. Natural hydraulic lime with a density of 2700 kg/m<sup>3</sup>, river natural sand with a density of 2322 kg/m<sup>3</sup>, superplasticizer (SP) Master SKY617 with a density of 1041 kg/m<sup>3</sup>, high workability class, a low W/C ratio, and distilled water were used to obtain the mortar pastes. Prismatic specimens with dimensions of 40 mm × 40 mm × 160 mm were produced to perform the mechanical tests. A control sample with no incorporation of  $OW_A$  was also produced for comparison purposes. The production of the mortar samples is exemplified in Figure 6.



**Figure 6.** Production of  $OW_A$  mortars: (a)  $OW_A$ ; (b) molding phase; (c) prismatic specimens after demolding and curing.

Three specimens of cement-based solid blocks and three specimens of lime mortars were produced for each formulation and subjected to flexural strength tests. In the case of

mortars, the samples resulting from the flexural test were used to perform the compressive analysis. A particleboard sample was enough to perform the thermal performance experiments in accordance with the standard procedure. All specimens were subjected to a curing process under the ambient conditions of the laboratory. The experimental tests were carried out after 28 days of curing in the case of mortars and particleboards, while blocks were tested after 300 days of curing.

### 3. Experimental Tests

#### 3.1. Flexural and Compression Tests

The solid block specimens were subjected to mechanical tests for flexural strength characterization at 300 days of curing, following the procedure indicated in standard EN 1015-11: 2019 [42]. In this case, the recommend values for 28 days of curing served as a reference for the results obtained at the age of 300 days. The results of flexural behavior at 300 days will be useful for further comparison with the ones obtained from the durability tests, which are part of a more detailed, ongoing investigation. The flexural strength was determined by three-point loading of the prismatic specimens until failure, with a speed of  $50 \pm 10$  N/s. Data related to the applied load in (kN) and displacement in (mm) were acquired for the further calculation of the flexural strength.

Flexural and compression tests were performed for the lime–mortars specimens at 28 days of curing, in accordance with standard EN 1015-11: 2019 [42]. For the compression strength determination, the two samples resulting from the flexural test were used for each paste formulation.

The flexural strength ( $f$ ) of the blocks and mortars, in  $\text{N}/\text{mm}^2$ , was calculated by applying Equation (1):

$$f = 1.5 \times \frac{F \times l}{b \times d^2} \quad (1)$$

where  $f$  is the maximum load applied to the specimen (in N),  $l$  is the distance between the support rollers (in mm),  $b$  is the width of the specimen (in mm), and  $d$  is the depth of the specimen (in mm). The mean value was calculated, and units were converted to MPa.

In the case of the mortar samples, the mean value of the compressive strength was achieved by dividing the maximum load carried by each specimen by its cross-sectional area.

#### 3.2. Thermal Performance Assessment

Regarding the particleboard with  $\text{OW}_5$ , thermal performance was evaluated according to ISO 9869 [43], and investigations were developed by Pereira [44] e Leitão et al. [45]. A multilayer solution, composed of a 20 mm  $\text{OW}_5$  particleboard and a plasterboard with 13 mm of thickness, was considered for performing the experimental test. Although it is possible to obtain a relatively homogeneous particleboard when the mixture with PVA included 83% olive stone, it was decided to estimate the thermal performance of the particleboard when placed together with a supporting or adjacent element. On the one hand, this fixation to another element makes it possible to avoid heat transfer through areas that are more heterogeneous in terms of composition, including possible voids or areas with PVA concentrations that could compromise the experimental results. On the other hand, the production of these types of particleboards involves their application to a support, serving as a covering element or filling material, functioning as the core of a multilayer element. Therefore, for simplicity, the board was glued only at its ends to a plasterboard sheet. This preparation of the sample also allowed us to verify that  $\text{OW}_5$  particleboards can be easily fixed to other elements, composing a multilayer element. The thermal performance of the particleboards was performed in a temperature-controlled test room with dimensions of  $4.00 \text{ m} \times 3.00 \text{ m} \times 2.54 \text{ m}$ . The sample was placed on the north façade, surrounded by extruded polystyrene (XPS) boards, and affixed using polyurethane foam (PU) to avoid thermal bridges, non-insulated headers, and other faults that could compromise the results. The surface containing  $\text{OW}_5$  was turned inward (Figure 7a), and the one with the plasterboard faced outward (Figure 7b).

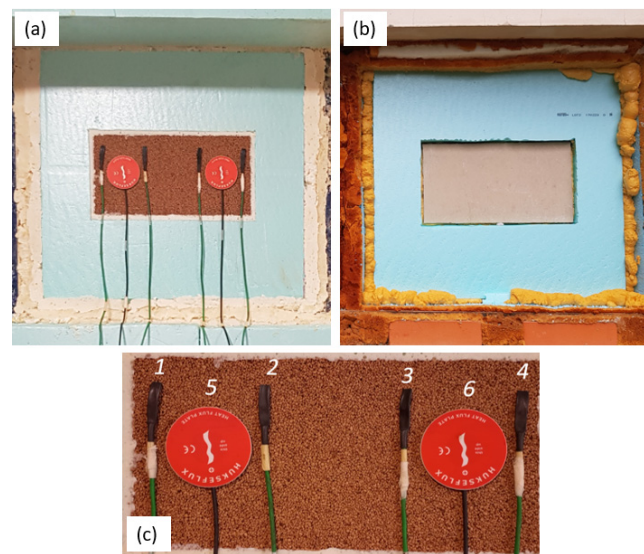


**Figure 7.** Experimental setup for the thermal performance assessment of  $OW_S$  particleboard solution: (a) interior view; (b) exterior view; (c) sensor's location in the  $OW_S$  particleboard: inner surface temperature sensors: 1— $Tsi_{11}$ , 2— $Tsi_{12}$ , 3— $Tsi_{21}$ , and 4— $Tsi_{22}$ ; heat flux sensors: 5— $HF_1$  and 6— $HF_2$ .

The thermal performance characterization of the of  $OW_S$  particleboard multilayer solution was based on the measurement of heat fluxes and inner surface temperatures values. Hygrothermal conditions of indoor and outdoor environments were also registered. The acquired data allowed us to estimate the thermal transmission coefficient of the composed solution. Two heat flux sensors,  $HF_1$  and  $HF_2$ , were affixed to the  $OW_S$  particleboard surface to measure variations in  $q_1$  and  $q_2$ , respectively, and four thermocouples were also used to measure inner surface temperatures  $Tsi_{11}$ ,  $Tsi_{12}$ ,  $Tsi_{21}$ , and  $Tsi_{22}$ , respectively (Figure 7c). Two temperature probes were placed inside and outside the test room to measure  $T_i$  and  $T_e$ , respectively. These values were measured with a time interval of 10 min.

According to ISO 9869 [43], a high thermal gradient between the interior of the test room and the exterior environment is desirable to guarantee a significant heat flow through the sample. Furthermore, a heat flux occurring in the same direction during the entire measurement period should also be guaranteed. In order to achieve these required conditions, a heating device was placed inside the test room to guarantee that the  $T_i$  value remained higher than  $T_e$ . The measurement period occurred between the 15th and the 30th of September. As mentioned previously, a continuous measurement of these values allowed us to estimate the thermal transmission coefficient ( $U$ ) of the  $OW_S$  multilayer solution applying Equation (1). In this equation, the heat flow,  $q(n)$ , at the instant  $n$ , measured by the  $HF$  sensor, occurs when a temperature differential between  $T_i(n)$  and  $T_e(n)$ , measured at the instant  $n$ , is guaranteed. According to ISO 9869 [43], it is recommended to use the values of the interior and exterior temperatures instead of the inner surface temperatures for calculating the  $U$  value. Equation (2) was applied twice, given that two heat flux sensors,  $HF_1$  and  $HF_2$ , were fixed in the sample's inner surface, allowing us to obtain two values of  $U'(ntotal)$ , defined as  $U1(ntotal)$  and  $U2(ntotal)$ . The average value of  $U1(ntotal)$  and  $U2(ntotal)$  leads to the final value of the thermal transmission coefficient, as indicated in Equation (3).

$$U(ntotal) = \frac{\sum_{n=1}^{ntotal} q(n)}{\sum_{n=1}^{ntotal} (T_i(n) - T_e(n))} \quad (2)$$

$$U'(ntotal) = \frac{U1(ntotal) + U2(ntotal)}{2} \quad (3)$$



Based on the experimental assessment of  $U'(ntotal)$  for the multilayer solution, it was possible to estimate the thermal resistance  $R'(ntotal)$  of the proposed building solution using Equation (4).

$$R'(ntotal) = \frac{1}{U'(ntotal)} \quad (4)$$

Considering the external and internal superficial thermal resistances,  $R_{se}$  and  $R_{si}$ , respectively, it is possible to obtain the thermal resistance of the multilayer solution, composed of the 20 mm  $OW_S$  particleboard and a plasterboard with 13 mm of thickness. Considering  $R_{OWS}$  as the thermal resistance of the particleboard,  $R_{plast}$  as the thermal resistance of the plasterboard,  $R_{se}$  as the inner surface thermal resistance, and  $R_{si}$  as the outer surface thermal resistance, Equation (5) allows us to determine  $R_{OWS}$ . In this case, the values of  $R_{se}$ ,  $R_{si}$ , and  $R_{plast}$  are  $0.04 \text{ m}^2\text{°C/W}$ ,  $0.13 \text{ m}^2\text{°C/W}$ , and  $0.052 \text{ m}^2\text{°C/W}$ , respectively [46].

$$R'(ntotal) = R_{OWS} + R_{plast} + R_{Si} + R_{Se} \quad (5)$$

The determination of  $R_{OWS}$  will lead to a theoretical approach to the thermal conductivity value of  $\lambda_{OWS}$  applying Equation (6), where  $e_{OWS}$  represents the thickness of the  $OW_S$  particleboard.

$$\lambda_{OWS} = \frac{e_{OWS}}{R_{OWS}} \quad (6)$$

## 4. Results and Discussion

### 4.1. Solid Blocks

Flexural tests were carried out for different formulations of solid blocks, considering two possible directions of application (horizontal and vertical). The results are presented in Figure 8. The results obtained at 300 days lead to the conclusion that an increase in waste content results in a decrease in flexural strength. Furthermore, as observed in Figure 8c, blocks with 5%  $OW_B$  present different values of strength in the two directions, showing a higher one in the vertical position due to increased inertia when compared to the horizontal position. However, an increase to 20% waste leads to significantly lower values of strength, and no representative difference is identified, depending on the position of the block when subject to the mechanical test.

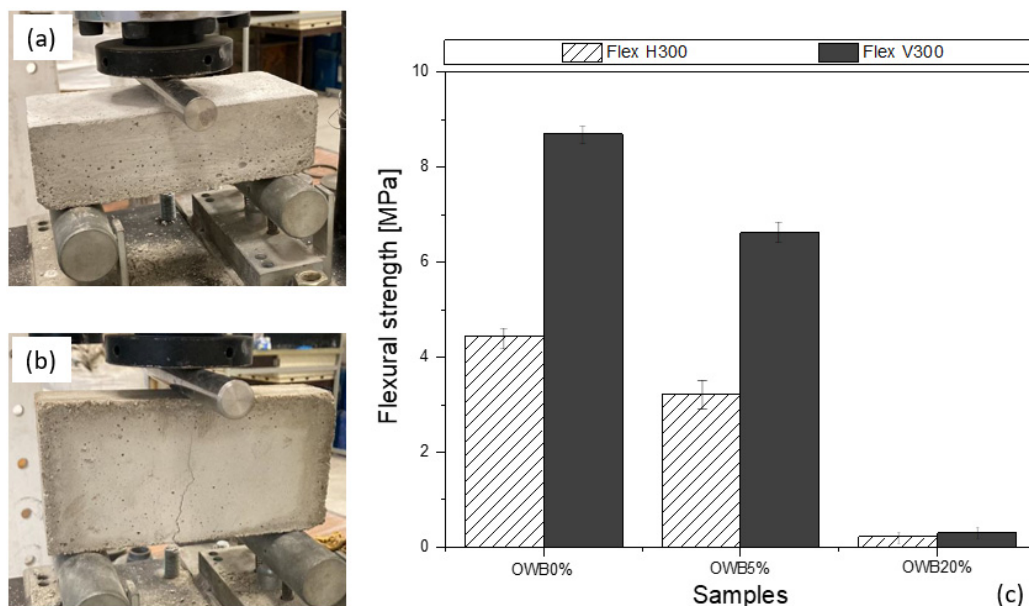


**Figure 8.** Flexural test of solid blocks with  $OW_B$  at 300 days of curing: (a) experimental procedure in the horizontal position; (b) failure mode of solid blocks with 5%  $OW_B$  in the vertical position; (c) flexural strength results in the vertical (V) and horizontal (H) positions.

Considering the establishments in the standard EN 772-13 [47], a minimum flexural strength of  $1.5 \text{ N/mm}^2$  is specified for concrete masonry units at 28 days of curing. Taking this value as a reference for a period of 300 days, blocks with 5%  $OW_B$  comply with the standard, while in the case of a 20% waste addition, the strength of the blocks significantly decreases, not allowing the fulfilment of these requirements.

In comparison with some studies related to the production of blocks incorporating different types of agricultural wastes, Sathiparan et al. [48] studied several compositions of blocks with agricultural wastes using rice husk, saw dust, peanut shell, rice straw, and coconut shell, whose results showed flexural strength values between 0.1 and 1.7 MPa for density values between  $900\text{--}1990 \text{ kg/m}^3$ . Regarding the use of bottom ash as a cement replacement, Wongkeo et al. [49] obtained solid blocks with flexural strengths between 2.6 and 4 MPa. Thus, it can be concluded that the results presented by  $OW_B$  solid blocks with 5% content are in accordance with those achieved by other authors when agricultural wastes are incorporated into mixtures. The obtained results also indicate the possibility of using wet bagasse to produce solid blocks for non-structural purposes, such as partition walls. However, given the decrease in mechanical performance verified at the percentage of 20%, optimization of the maximum content of  $OW_B$  is required.

#### 4.2. Particleboards

The particleboards containing  $OW_S$  were subjected to an experimental analysis of thermal performance, allowing us to obtain the heat flux variation and the corresponding thermal performance coefficient. Indoor and outdoor temperatures were also continuously measured, allowing us to obtain the variation in  $T_i$  and  $T_e$  values. Figure 9 presents the values acquired by the two heat flux sensors,  $q_1(h)$  and  $q_2(h)$ , during the measurement period. The values of the interior ( $T_i$ ) and exterior ( $T_e$ ) temperature are also represented, showing that indoor temperatures were always higher than exterior temperatures, as required to ensure the reliability of the results. Stabilization of the interior temperature was guaranteed for almost the entire period, except between 20 and 21 September, characterized by an increase in  $T_i$  values, which was due to an uncontrolled change in the heating device located inside the test room. However, given that this situation occurred during a very short period compared to the entire measurement period, it can be considered negligible.

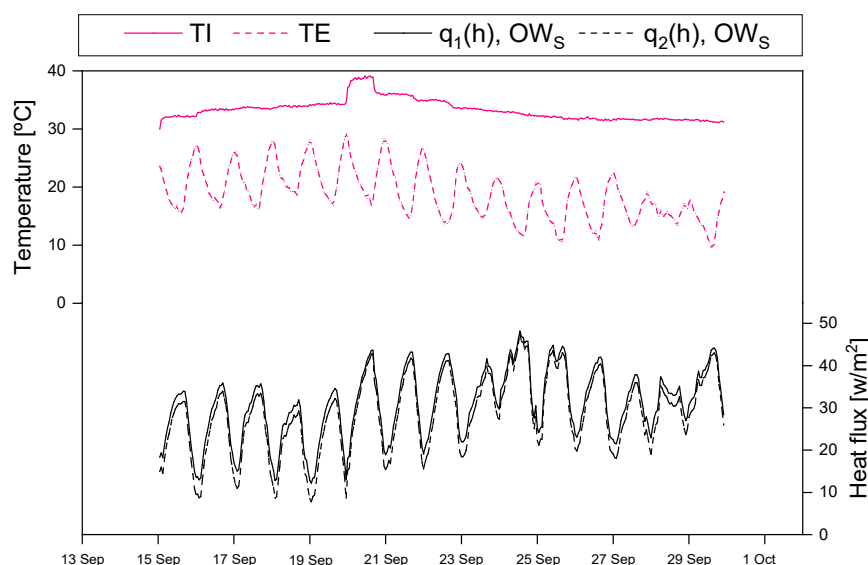


**Figure 9.** Heat flux variations of the  $OW_S$  particleboard solution.

A minimum value of  $5.3 \text{ W/m}^2$  during the night and a maximum of  $49.5 \text{ W/m}^2$ , during the day were achieved for heat fluxes for the multilayer solution. Given the two curves obtained by heat flux sensors  $HF_1$  and  $HF_2$ , it is possible to observe the similarity in

the curve's development, which may be representative of the homogeneity of the surfaces where the respective sensors were fixed.

The variation of inner surface temperatures was also measured. Given that the values obtained by sensors  $T_{si11}$  and  $T_{si12}$  and  $T_{s21}$  and  $T_{s22}$  are quite close, Figure 10 only presents the average values, designated as  $T_{si1}$  and  $T_{si2}$ , respectively. As expected, the surface temperature curves are similar to those obtained for heat flux and present values lower than those obtained for the temperature of the test room. A variation of the curve's amplitude is visible, with lower  $T_{si2}$  values, which may be related to an area with a higher PVA concentration, which presents a higher thermal conductivity compared to  $OW_S$ . However, this differential corresponds to a maximum of 1.9 °C and a minimum of 0.3 °C. Regarding the mean values obtained by the sensors,  $T_{si1}$  achieved a minimum of 26.5 °C and a maximum of 36.1 °C, while for  $T_{si2}$ , these values were 26.2 °C and 35.0 °C, respectively.

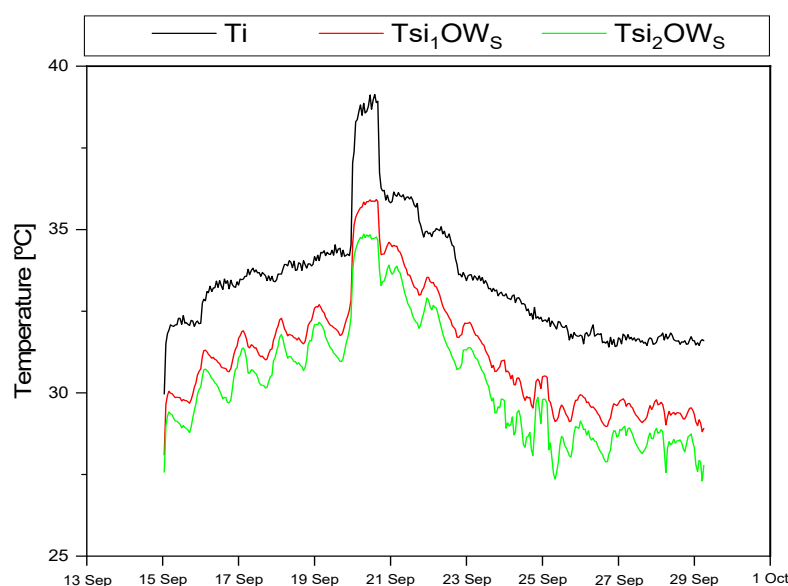


**Figure 10.** Variation of the inner surface ( $T_{si}$ ) and interior ( $T_i$ ) temperatures of the  $OW_S$  particleboard solution.

As mentioned previously, the tested solution was composed of an  $OW_S$  particleboard and a plasterboard with 13 mm of thickness. The results acquired by heat flux sensors and the temperatures of the interior and exterior environments were used to estimate the thermal transmission coefficient of the solution. It is possible to conclude that adding a 20 mm  $OW_S$  particleboard to the plasterboard with 13 mm leads to a value of 2.12 W/m<sup>2</sup>°C. Furthermore, this experimental analysis also demonstrates the possibility of producing particleboards using olive stone with integrity and dimensional stability, making them capable of being affixed to other materials and easily integrated into a multilayer solution.

The application of Equations (3)–(5) allowed us to estimate a thermal conductivity value of 0.08 W/mK for the  $OW_S$  particleboard.

A comparison of the obtained results with the ones already known for commercial and innovative building solutions was also performed. As seen in Table 4, the incorporation of olive stone as an aggregate for particleboards shows promising properties regarding thermal insulation applications, namely for covering interior walls.

#### 4.3. Mortars

Flexural and compression tests were carried out for different formulations of lime–mortars, whose results can be observed in Figure 11. The results reveal that the incorporation of 2%  $OW_A$  leads to an increase in the mechanical properties of the lime–mortars when compared to the reference mortar with no ash addition. If the proportion of waste content in the mixture is changed to 8%, the values of flexural and compressive strength

decrease compared with the solution containing 2% waste. However, in this case, the value of compression strength is relatively close to the one obtained for the lime–mortar with no incorporation of olive stone ash, revealing that incorporating an intermediate percentage of  $OW_A$  can result into a mechanical performance improvement. According to the standard EN 998-1:2010 [51], all mortars can be classified in category CS II (compressive strength between 1.5 and 5.0 MPa at 28 days). These results suggest the possibility of applying these types of mortars as interior coatings for walls.

**Table 4.** Density and thermal conductivity of commercial and innovative insulation solutions.

| Insulation Materials                              | Density (kg/m <sup>3</sup> ) | Thermal Conductivity ( $\lambda$ ) (W/mK) |
|---|------------------------------|---|
| $OW_S$ Particleboard (material under study)       | 700                          | 0.08                                      |
| Expanded polystyrene (EPS) [46]                   | 15–20                        | 0.040                                     |
| Extruded polystyrene (XPS) [46]                   | 25–40                        | 0.037                                     |
| Polyisocyanurate/Polyurethane foam (PIR/PUR) [46] | 20–50                        | 0.040                                     |
| Wood fibre (rigid) [50]                           | 160                          | 0.0038                                    |
| Wood fibre (flexible) [50]                        | 50                           | 0.0038                                    |
| Mineral wool (MW) [46]                            | 100–150                      | 0.042                                     |
| Glass wool [46]                                   | 15–100                       | 0.040                                     |
| Black cork agglomerate [46]                       | 90–140                       | 0.045                                     |
| Hemp [50]   | 25–28                        | 0.039–0.040                               |

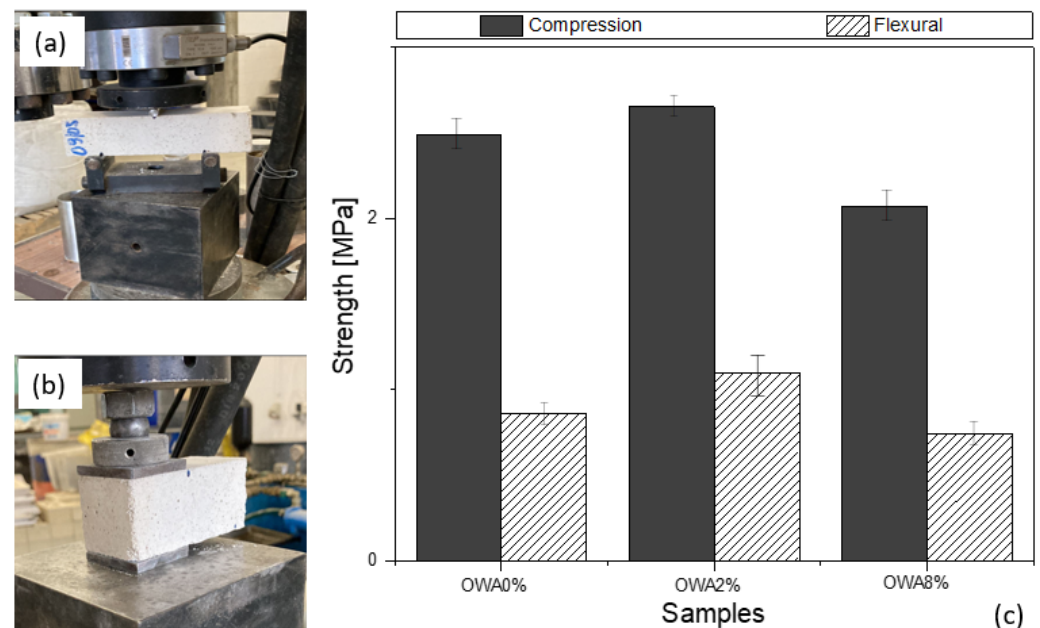


**Figure 11.** Flexural (a) and compression (b) experimental procedure for mortars; (c) strength results at 28 days of curing.

## 5. Conclusions

The possibility of introducing wastes and by-products originating from olive oil production as components of building materials was evaluated in this investigation. Wet bagasse was added into cementitious mixtures at percentages of 5% and 20% to produce solid blocks, ash was incorporated at percentages of 2% and 8% to develop lime–mortars, and 83% olive stone was mixed with polyvinyl acetate to produce particleboards. The obtained results lead to the following conclusions:

- Incorporating 5% wet bagasse in the composition of solid blocks allowed us to comply with standard requirements for flexural strength, whose value significantly decreases with a content of 20%;



- Adding 2% and 8% ash into lime–mortars pastes results in the accomplishment of standard values for flexural and compressive strength. It was also observed that the incorporation of 2% ash increased the mechanical properties of the proposed mortars when compared to a reference mortar with no ash addition;
- Affixing a 20 mm particleboard with 83% olive stone to a plasterboard with 13 mm thickness allowed us to obtain a multilayer solution with a thermal transmission coefficient of  $2.12 \text{ W/m}^2\text{°C}$ , showing promising thermal properties when compared to some conventional building solutions.

Thus, the wastes and by-products resulting from the olive oil production processes present potential for valorization as building material components for non-structural purposes. Although the results obtained reveal their possibility of being used as building materials components, more investigation is required concerning the chemical and physical properties of the different residues, as well as mechanical, thermal, acoustic, and durability characteristics of the originated composites materials, in order to optimize formulations and identify the most suitable applications.

**Author Contributions:** Conceptualization, A.B.-S. and A.J.; methodology, A.B.-S. and A.J.; validation, A.B.-S.; formal analysis, A.B.-S. and A.J.; investigation, A.B.-S., M.F. and A.J.; resources, A.B.-S., M.F. and A.J.; data curation, A.B.-S., M.F. and A.J.; writing—original draft preparation, A.B.-S. and A.J.; writing—review and editing, A.B.-S.; visualization, A.B.-S.; supervision, A.B.-S. and M.F.; project administration, A.B.-S. and M.F.; funding acquisition, A.B.-S. and M.F. All authors have read and agreed to the published version of the manuscript.

**Funding:** This work was funded by project I&D&I OBtain, operation No. NORTE-01-0145-FEDER-000084, co-financed by the European Regional Development Fund (FEDER) through NORTE 2020 (Northern Regional Operational Program 2014/2020), and CQ-VR, supported by FCT through the projects UIDB/00616/2020 and UIDP/00616/2020. M. Fernandes acknowledges FCT-UTAD for the contract in the scope of Decree-Law No. 57/2016–Law No. 57/2017.

**Data Availability Statement:** The raw data supporting the conclusions of this article will be made available by the authors on request.

**Conflicts of Interest:** The authors declare no conflicts of interest.

## References

1. Nations, U. População Mundial Atinge os Oito Mil Milhões em Novembro. 2022. Available online: <https://unric.org/pt/populacao-mundial-atinge-os-oito-mil-milhoes-em-novembro/> (accessed on 14 April 2023).
2. Briga-Sá, A.; Teixeira, J.; Jerónimo, A.; Fernandes, M. The influence of Olive Bagasse on the Heat of Hydration of Ordinary Portland Cement Pastes based on Infrared Thermography Analysis. In Proceedings of the ICEUBI2022—International Congress on Engineering—Innovation and Sustainability Praxis, Covilhã, Portugal, 28–30 November 2022.
3. Madurwar, M.V.; Ralegaonkar, R.V.; Mandavgane, S.A. Application of agro-waste for sustainable construction materials: A review. *Constr. Build. Mater.* **2013**, *38*, 872–878. [CrossRef]
4. Maraveas, C. Production of sustainable construction materials using agro-wastes. *Materials* **2020**, *13*, 262. [CrossRef]
5. Khan, R.; Jabbar, A.; Ahmad, I.; Khan, W.; Khan, A.N.; Mirza, J. Reduction in environmental problems using rice-husk ash in concrete. *Constr. Build. Mater.* **2012**, *30*, 360–365. [CrossRef]
6. Kanning, R.C.; Portella, K.F.; Bragança, M.O.; Bonato, M.M.; Santos, J.C.D. Banana leaves ashes as pozzolan for concrete and mortar of Portland cement. *Constr. Build. Mater.* **2014**, *54*, 460–465. [CrossRef]
7. Frías, M.; Savastano, H.; Villar, E.; de Rojas, M.I.S.; Santos, S. Characterization and properties of blended cement matrices containing activated bamboo leaf wastes. *Cem. Concr. Compos.* **2012**, *34*, 1019–1023. [CrossRef]
8. Singh, N.; Das, S.; Singh, N.; Dwivedi, V. Hydration of bamboo leaf ash blended Portland cement. *Indian J. Eng. Mater. Sci.* **2007**, *14*, 69–76.
9. Singh, N.; Singh, V.; Rai, S. Hydration of bagasse ash-blended portland cement. *Cem. Concr. Res.* **2000**, *30*, 1485–1488. [CrossRef]
10. Kazmi, S.M.S.; Abbas, S.; Munir, M.J.; Khitab, A. Exploratory study on the effect of waste rice husk and sugarcane bagasse ashes in burnt clay bricks. *J. Build. Eng.* **2016**, *7*, 372–378. [CrossRef]
11. Dungani, R.; Karina, M.; Sulaeman, A.; Hermawan, D.; Hadiyane, A. Agricultural waste fibers towards sustainability and advanced utilization: A review. *Asian J. Plant Sci.* **2016**, *15*, 42–55. [CrossRef]
12. Ghavami, K. Bamboo as reinforcement in structural concrete elements. *Cem. Concr. Compos.* **2005**, *27*, 637–649. [CrossRef]
13. Li, Y.; Mai, Y.-W.; Ye, L. Sisal fibre and its composites: A review of recent developments. *Compos. Sci. Technol.* **2000**, *60*, 2037–2055. [CrossRef]

14. Mo, K.H.; Thomas, B.S.; Yap, S.P.; Abutaha, F.; Tan, C.G. Viability of agricultural wastes as substitute of natural aggregate in concrete: A review on the durability-related properties. *J. Clean. Prod.* **2020**, *275*, 12306. [CrossRef]
15. Bories, C.; Aouba, L.; Vedrenne, E.; Vilarem, G. Fired clay bricks using agricultural biomass wastes: Study and characterization. *Constr. Build. Mater.* **2015**, *91*, 158–163. [CrossRef]
16. Cintura, E.; Nunes, L.; Esteves, B.; Faria, P. Agro-industrial wastes as building insulation materials: A review and challenges for Euro-Mediterranean countries. *Ind. Crops Prod.* **2021**, *171*, 113833. [CrossRef]
17. de Azevedo, A.R.; Amin, M.; Hadzima-Nyarko, M.; Agwa, I.S.; Zeyad, A.M.; Tayeh, B.A.; Adesina, A. Possibilities for the application of agro-industrial wastes in cementitious materials: A brief review of the Brazilian perspective. *Clean Mater.* **2022**, *3*, 100040. [CrossRef]
18. Liuzzi, S.; Sanarica, S.; Stefanizzi, P. Use of agro-wastes in building materials in the Mediterranean area: A review. *Energy Proc.* **2017**, *126*, 242–249. [CrossRef]
19. Shafigh, P.; Mahmud, H.B.; Jumaat, M.Z.; Zargar, M. Agricultural wastes as aggregate in concrete mixtures: A review. *Construct. Build. Mater.* **2014**, *53*, 110–117. [CrossRef]
20. Olive, S. Importance of the Olive Grove in the Mediterranean Basin. 2022. Available online: <https://sustainolive.eu/importance-olive-grove-mediterranean-basin/?lang=en> (accessed on 14 April 2023).
21. Laajine, H.O.F.; El Yamani, M.; El Hilaly, J.; Rharrabti, Y.; Amarouch, M.Y.; Mazouzi, D. Olive mill solid waste characterization and recycling opportunities: A review. *J. Mater. Environ. Sci.* **2017**, *8*, 2632–2650.
22. NE. Produção de Azeitona (t) por Local de Proveniência da Azeitona (Região Agrária). 2022. Available online: [https://www.ine.pt/xportal/xmain?xpid=INE&xpgid=ine\\_indicadores&indOcorrCod=0000705&selTab=tab0&xlang=pt](https://www.ine.pt/xportal/xmain?xpid=INE&xpgid=ine_indicadores&indOcorrCod=0000705&selTab=tab0&xlang=pt) (accessed on 14 April 2023).
23. Soares, B.M. *Pré-Tratamentos Aquosos do Bagaço e Caroço de Azeitona para Obtenção de Compostos de Valor Acrescentado*; Universidade de Lisboa: Lisboa, Portugal, 2019. (In Portuguese)
24. Solé, M.M.; Pons, L.; Conde, M.; Gaidau, C.; Bacardit, A.J.M. Characterization of wet olive pomace waste as bio based resource for leather tanning. *Materials* **2021**, *14*, 5790. [CrossRef] [PubMed]
25. Klisovic, D.; Novoselic, A.; Jambrak, A.R.; Brkic, K. The utilisation solutions of olive mill by-products in the terms of sustainable olive oil production: A review. *Int. J. Food Sci. Technol.* **2021**, *56*, 4851–4860. [CrossRef]
26. Tayeh, B.A.; Hadzima-Nyarko, M.; Zeyad, A.M.; Al-Harazin, S.Z. Properties and durability of concrete with olive waste ash as a partial cement replacement. *Adv. Concr. Construct.* **2021**, *11*, 59.
27. Al-Akhras, N.M.; Abdulwahid, M. Utilisation of olive waste ash in mortar mixes. *Struct. Concr.* **2010**, *11*, 221–228. [CrossRef]
28. Al-Akhras, N.M.; Attom, M.F.; Al-Akhras, K.M. Performance of olive waste ash concrete exposed to thermal cycling. *J. ASTM Int.* **2010**, *7*, 1–11.
29. Cuenca, J.; Rodriguez, J.; Martín-Morales, M.; Sanchez-Roldan, Z.; Zamorano, M. Effects of olive residue biomass fly ash as filler in self-compacting concrete. *Construct. Build. Mater.* **2013**, *40*, 702–709. [CrossRef]
30. Beltran, M.G.; Barbudo, A.; Agrela, F.; Jimenez, J.R.; de Brito, J. Mechanical performance of bedding mortars made with olive biomass bottom ash. *Construct. Build. Mater.* **2016**, *112*, 699–707. [CrossRef]
31. Cruz-Yusta, M.; Marmol, I.; Morales, J.L. Sanchez Use of olive biomass fly ash in the preparation of environmentally friendly mortars. *Environ. Sci. Technol.* **2011**, *45*, 6991–6996. [CrossRef] [PubMed]
32. Cheraghalizadeh, R.; Akçaoğlu, T. Properties of self-compacting concrete containing olive waste ash. *Cem. Lime Concr.* **2020**, *25*, 178–187. [CrossRef]
33. Barreca, F.; Fichera, C.R. Use of olive stone as an additive in cement lime mortar to improve thermal insulation. *Energy Build.* **2013**, *62*, 507–513. [CrossRef]
34. Sutcu, M.; Ozturk, S.; Yalamac, E.; Gencel, O. Effect of olive mill waste addition on the properties of porous fired clay bricks using Taguchi method. *J. Environ. Manag.* **2016**, *181*, 185–192. [CrossRef]
35. Eliche-Quesada, D.; Leite-Costa, J. Use of bottom ash from olive pomace combustion in the production of eco-friendly fired clay bricks. *Waste Manag.* **2016**, *48*, 323–333. [CrossRef]
36. Abdeliazim, M.; Bassam, A.; Yazan, I.; Musab, S. Utilising olive-stone biomass ash and examining its effect on green concrete: A review paper. *J. Mater. Res. Technol.* **2023**, *24*, 7091–7107.
37. Boukhari, M.; Merroun, O.; Maalouf, C.; Bogard, F.; Kissi, B. Exploring the impact of partial sand replacement with olive waste on mechanical and thermal properties of sustainable concrete. *Clean. Mater.* **2023**, *9*, 2772–3976. [CrossRef]
38. Boukhari, M.; Merroun, O.; Maalouf, C.; Bogard, F.; Kissi, B. Comprehensive experimental study on mechanical properties of a structural concrete lightened by olive pomace aggregates mixed with olive mill wastewater. *World J. Eng.* **2023**, preprint. [CrossRef]
39. Boukhari, M.; Merroun, O.; Maalouf, C.; Bogard, F.; Kissi, B. Experimental investigation on the mechanical strength and thermal conductivity of concrete lightened by olive mill solid waste. *Mater. Today Proceed.* **2023**. [CrossRef]
40. Farag, E.; Alshebani, M.; Elhrrari, W.; Klash, A.; Shebani, A. Production of particleboard using olive stone waste for interior design. *J. Build. Eng.* **2020**, *29*, 2352–2710. [CrossRef]
41. Jerónimo, A.; Briga-Sá, A.; de Zea Bermudez, V.; Nunes, S.C.; Fernandes, M. Physico-chemical characterization of olive oil production residues: Valorization as building materials. In Proceedings of the Construção, Guimarães, Portugal, 5–7 December 2022.

42. NP EN 1015-11; Methods of Test for Masonry—Part 11: Determination of Flexural and Compressive Strength of Hardened Mortar. European Committee for Standardization (CEN): Brussels, Belgium, 2019.
43. ISO 9869; Thermal Insulation—Building Elements—In-Situ Measurement of Thermal Resistance and Thermal Transmittance. International Organization for Standardization (ISO): Geneva, Switzerland, 1994.
44. Cunha, S. In Situ Evaluation and Certification of the Thermal Quality of Residential Buildings. Ph.D. Thesis, UTAD, Vila Real, Portugal, 2011.
45. Leitão, D.; Barbosa, J.; Soares, E.; Miranda, T.; Cristelo, N.; Briga-Sá, A. Thermal performance assessment of masonry made of ICEB's stabilised with alkali-activated fly ash. *Energy Build.* **2017**, *139*, 44–52. [[CrossRef](#)]
46. Santos, C.; Matias, L. *Coeficientes de Transmissão Térmica de Elementos da Envolvente dos Edifícios*; Coleção Edifícios—ITE 50: Lisbon, Portugal, 2006; ISBN 978-972-49-2065-8.
47. EN 772-13; Methods of Test for Masonry Units—Part 13: Determination of Net and Gross Dry Density of Masonry Units (Except for Natural Stone). European Committee for Standardization (CEN): Brussels, Belgium, 2000.
48. Sathiparan, N.; De Zoysa, H. The effects of using agricultural waste as partial substitute for sand in cement blocks. *J. Build. Eng.* **2018**, *19*, 216–227. [[CrossRef](#)]
49. Wongkeo, W.; Thongsanitgarn, P.; Pimraksa, K.; Chaipanich, A.J.M. Design, Compressive strength, flexural strength and thermal conductivity of autoclaved concrete block made using bottom ash as cement replacement materials. *Mater. Des.* **2012**, *35*, 434–439. [[CrossRef](#)]
50. Greenspec. Insulation Materials and Their Thermal Properties. 2018. Available online: <http://www.greenspec.co.uk/building-design/insulation-materials-thermal-properties/> (accessed on 23 October 2023).
51. NP EN 998-1; Specification for Mortar for Masonry—Part 1: Rendering and Plastering Mortar. European Committee for Standardization (CEN): Brussels, Belgium, 2010.

**Disclaimer/Publisher's Note:** The statements, opinions and data contained in all publications are solely those of the individual author(s) and contributor(s) and not of MDPI and/or the editor(s). MDPI and/or the editor(s) disclaim responsibility for any injury to people or property resulting from any ideas, methods, instructions or products referred to in the content.